Free Radical Polymerization of Acrylic Acid at High Monomer Concentration in a Continuous Flow Reactor

by

Sugandhika Samdhian

Bachelor of Engineering in Chemical Engineering, Panjab University, India, 2017

Submitted to the Graduate Faculty of the

Swanson School of Engineering in partial fulfillment

of the requirements for the dual degree of

Master of Science

University of Pittsburgh

2022

UNIVERSITY OF PITTSBURGH

SWANSON SCHOOL OF ENGINEERING

This thesis was presented

by

Sugandhika Samdhian

It was defended on

November 4, 2022

and approved by

Lei Li, PhD, Associate Professor, Department of Chemical and Petroleum Engineering

Susan Fullerton, PhD, Grad Chair and Associate Professor, Department of Chemical and Petroleum Engineering

Thesis Advisor: Dr. Sachin Velankar, PhD, Professor, Department of Chemical and Petroleum Engineering

Free Radical Polymerization of Acrylic Acid at high monomer concentration in a Continuous Flow Reactor

Sugandhika Samdhian, MS

University of Pittsburgh, 2022

Most of the world's polyacrylic acid (PAA) is produced by batch or semi-batch processes. In the case of free-radical polymerization (FRP), continuous processes may offer advantages concerning safety, productivity, product quality, and cost. Designing a continuous process for a polymer with a high total polymer concentration imposes challenges like its likelihood of polymer deposition on the walls of the reactor, and runaway reactions, which were addressed in this work. In addition, a continuous lab-scale process using a tubular reactor was evaluated for the polymerization of acrylic acid in an aqueous solution to transition from the batch to continuous flow production of high monomer content or total solid (TS) polyacrylic acid with the aim of meeting product specifications 300,000 g/mol molecular weight, a polydispersity of 10 or below, and PAA concentration of 25% with ≥99% conversion. The feasibility of producing waterborne polyacrylic acid with ammonium persulfate via a lab-scale continuous-flow tubular reactor was investigated experimentally. Initially, the FlowSyn microreactor (Uniqsis Ltd., United Kingdom) was used for experimentation but was replaced by a two-monomer feed tubular configuration. These lab-scale data provided experimental and theoretical bases for process scale-up to the pilot-scale plant. The thesis also includes a literature review discussing various approaches to establish a way to safely switch from the discontinuous to the continuous flow process for the production of polyacrylic acid.

Table of Contents

List of Tables

List of Figures

Preface

This thesis is the final work as partial fulfillment of my master’s program at the Swanson School of Engineering, University of Pittsburgh. It serves as the documentation of my research at Pitt and my time at Lubrizol as a visiting researcher. This thesis presents the results of a study toward establishing a safe transit from batch to continuous flow production of high monomer content polyacrylic acid.

This project was done under the guidance of Dr. Sachin Velankar and Dr. Lei Li in the Department of Chemical and Petroleum Engineering, University of Pittsburgh, between January 2021 to September 2022. A portion of the research was done under the guidance of John Dietrich at Lubrizol, Avon OH, between July 2022 to August 2022.

Acknowledgement

Foremost, I am sincerely thankful to my advisors, Dr. Sachin Velankar and Dr. Lei Li, for their guidance and constant support throughout this project. I am also grateful for the provision of laboratory facilities in the Department of Chemical and Petroleum Engineering, University of Pittsburgh. I am grateful to my advisors for their endless efforts, knowledge, and enthusiasm, without which this project would not have been possible.

I would like to acknowledge the tremendous support from John Dietrich and Glenn Cormack at Lubrizol. The team at Lubrizol has provided their constant input and guidance and provided me with an opportunity to work at their excellent research facility in Avon, OH. I would like to extend my thanks to Kyle Oliva for his assistance during my time at Lubrizol.

I would also like to express my gratitude to Joshua Ward for sharing his experiences and learnings from the preceding research.

This research would not have been possible without Lubrizol's financial support and their strong partnership with the University of Pittsburgh.

1.0 Introduction

Polyacrylic Acid (PAA) is a high molecular weight polymer with growing global demand. According to the Global Polyacrylic Acid Market Research Report 2021, the worldwide Polyacrylic Acid market was worth US$ 476.9 million in 2019, and that is predicted to reach US$ 706 million by the end of 2026, increasing at a compound annual growth rate (CAGR) of 5.7% during 2021-2026 [1]. They can be homopolymers of acrylic acid or crosslinked with an allyl ether of pentaerythritol, allyl ether of sucrose, or allyl ether of propylene that augment the market's growth. Many polymer characteristics determine PAA's application in many industrial sectors, for instance, polymer's molecular weight: (a) Molecular mass less than 20kDa (low molecular wt.) is used as sequestrant; (b) Molecular mass range between 20-80kDa (mid-low) are used in paints;(c) Molecular mass ranging within 0.1-1MDa (mid-high) is adopted in the textile and paper industry, and; (d) Polymers over the 1 MDa molecular weight range are used as flocculating agent and adsorbents for wastewater treatments [2-4]. Hence, controlling such factors as molecular weight distribution, dispersity index, and particle surface charge by adequately tuning the operational conditions potentially influences the market. In fact, in a polymer material, the polymer's microstructure determines the material's final properties, such as shear stress-strain curves, tensile strength, crystallinity, resilience, elasticity, and conductivity. Achieving control on such properties is crucial for determining the use of the polymer in daily applications and, thus, for efficient polymer production.

The PAA industrial-scale production typically relies on discontinuous (batch) or semicontinuous (semibatch) processes. The free-radical polymerization (FRP) reaction of AA is highly exothermic (63KJ/mol [5]), posing a potential risk to the safety of the production unit, if cooling fails, when discontinuous batch reactors (BR) are being used [5]. Moreover, accidents causing process failure due to thermal runaways are common during FRP [6]. Runaways are particularly likely in the discontinuous process scenario because of the reactor's large monomer hold-up and inefficient heat removal capability. Tubular reactors are relatively more effective than BR and semi-batch reactors (SBR) in thermal control because of their higher heat-exchange-surface-to-volume ratio [7]. In addition to improved safety from such potential risks, the transition towards a continuous process would bring a lower capital cost, ability to change grades rapidly, and enhanced sustainability [8, 9]. These considerations and the trend of the increasing PAA demand motivate manufacturers towards adopting continuous production. The European Union (EU) funded F3 factory (where F3 stands for flexible, fast, and future) is one of the most vivid examples with the same fundamental approach with about EUR 30 million budget [10].

Several methods are used to aid the transitioning from a BR or SBR to a continuous flow process by using modular stirring reactors or tubular reactors with adequately distributed side injections and static mixers[11-13]. Recently, tubular microreactors have been proved to be a valuable resource with many benefits for many polymers synthesis such as FRP, anion-cationic, and polycondensation [14]. A study on FRP of many polymers, including - butyl acrylate and methyl methacrylate, in a microreactor was conducted by Iwasaki and Yoshida [15]. According to the study, the data showed narrow molecular weight distribution of the polymers and the microreactor's effective heat removal ability. Moreover, the inbuilt features of a tubular microreactor, such as water jacketed coiled reaction tubes and micromixers, provide better control over reaction dynamics of the polymerization, which is, otherwise hard to attain [16]. The process conditions are designed to target the specific initiator process, desired molecular weight distribution, and conversion. Mainly, azo compounds (e.g., azobisisobutyronitrile), peroxides (e.g., benzoyl peroxide), and redox coupled persulfates are used as initiators [17].

However, some persistent hurdles make the transition from BR to continuous flow process difficult for high concentrations, such as clogging (accumulation of polymer in the reactor causing resistance in the flow); adiabatic temperature rise, and auto-acceleration due to Trommsdroff- Norrish gel effect. Therefore, polymer manufacturers interested in this transition put a lot of effort into process optimization to retain the same product profile [13].

The main goals of the thesis were 1) to safely transit from batch to continuous flow production of high monomer content PAA; 2) to produce PAA product using continuous flow that is of equivalent specs as the current batch process, and 3) to establish a thermally stable reaction that can produce PAA for long durations. Chapter 2 of this thesis is a literature review of all the research papers associated with the production of polyacrylic acid in a continuous-flow reactor. In Chapter 3, I have described the experimental setup & the materials used in the thesis work, and how the samples were characterized. Chapter 4 discusses the results of all the experiments conducted for the thesis work. Chapter 5 was for the discussion of what could be done in the future to optimize the process.

2.0 Literature Review

Author and Year	Title	Max. Total Solids %	Initiator	[I] concentration or wt.%	T (Celsius)	Method	CSTR/ Tubular	Mw (kg/mol)
Hashemi et al, 2013, [18]	Optimizing Control of a Continuous polymerization Reactor	20 (Model - predicted values)	Sodium Persulfate		80	A computer aided model was designed by using Model Predictive Control (MPC) that is discretized by Weight Essentially Non-Oscillatory (WENO) scheme. The controller is placed on the pilot plant setup to predict and manipulate the results, to optimize the production rate within the constraints of product quality.	Tubular reactors in series	77
Micic et al, 2014, [20]	Scale-up of the Reversible Addition-Fragmentation Chain Transfer (RAFT) Polymerization Using Continuous Flow Processing	17.7	4,4'-azobis (4-cyanovaleric acid)	0.45% w	80	Demonstrated a controlled radical polymerization process using RAFT reagent to scale up a small laboratory process of 5ml scale batch reactor to a 500 ml scale tubular reactor. The paper has also compared the stability of the ongoing reaction in both batch and continuous process by recording the temperature profile and corresponding concentration profile for different configurations.	Tubular reactor	23.2

Chevrel et al, 2016, [19]	Continuous Pilot-Scale Tubular Reactor for Acrylic Acid Polymerization in Solution Designed Using Lab-Scale Rheo-Raman data	10	Potassium persulfate	0.20%	60	A continuous pilot-scale tubular reactor with eight intermediate feeds was designed and investigated for the radical polymerization of acrylic acid in an aqueous solution. A mathematical model was established using material balance, reaction kinetics equations, and rheological parameters from a previous study by the same authors using a lab-scale rheo-Raman device.	PFR with intermediate feeds	1000
Qiu et al, 2016, [16]	Kinetic study of acrylic acid polymerization with a microreactor	10	KBS/ K2S2O8	0.028-0.112 M	95	The microreactor platform is used to study kinetics with more than 40ml/min flowrate	tubular microreactor	120-180
Brocken et al, 2017, [21]	Continuous flow synthesis of polyacrylic acid via free radical polymerization	0.01	2.2-azobis dihydrochloride	0.69mM	70-90	The free radical polymerization of aqueous AA solution was studied for different operational conditions using a FlowSyn reactor.	FlowSyn reactor	118-477
Florit et al, 2020, [11],	Solution Polymerization of acrylic acid initiated by redox couple Na-PS/Na-MBS: Kinetic model	10 (Model-predicted values for PFR)	Na-PS/Na-MBS	0.05-0.07 M	50- 90	A mathematical model was established using material balance and population density balance equations (MoM) for BR and SBR processes. The model was first validated for discontinuous reactors applying	PFR with intermediate feeds	-

	and transition to continuous process.					a set of varying reaction conditions and then made to predict polymer spec values for PFR with intermediate feeds for the same set of experiments. The mathematical model was applied to guide the transition from SBR to continuous PAA production while ensuring the same polymer content and final average molecular weight of semi batch process.		
Ilare et al, 2020, [13]	From batch to continuous free-radical solution polymerization of acrylic acid using a stirred tank reactor	20	Ammonium persulfate	0.2 to 1M	60-80	A mathematical model was established by using material balance and population density balance equations (MoM) for BR and SBR processes. The model first validated for discontinuous reactors using a set of varying reaction conditions and then for the continuous stirred reactor CSTR. The mathematical model applied to guide the transition from SBR to continuous PAA production while ensuring the same polymer content and final average molecular weight of semi batch process.	CSTR	500

Polymerization conducted in continuous flow offers several distinct advantages, including improved efficiency, reproducibility, and enhanced safety for exothermic polymerizations using highly toxic or corrosive components, high pressures, and temperatures. Since the continuous flow for radical polymerization offers such advantages, the number of reports using continuous flow processes for both tubular reactors and CSTR to perform polymerization has grown in recent years. The literature review section of this thesis focuses primarily on reviewing research papers (summarized in the above table) that have demonstrated successful transition of radical polymerization of acrylic acid in batch or semi-batch process to continuous flow technology and include selected examples that are relevant to this study. Not all these articles have conducted experiments on continuous reactors; some only have model predictions for continuous reactors.

One way of successfully shifting the process from batch to continuous process, which several papers have illustrated, is to develop a computer-aided mathematical model and apply it to control and optimize the polymer production. An example is the European F3- factory project (2009). A consortium of 25 partners, from nine EU countries, coordinated by industrial enterprises such as Bayer, BASF, and Evonik, and the scientific research institutes such as the Technical University of Dortmund and the RWTH Aachen University, has been working on this project since 2009 the development of standardized and modularized production systems for the chemical industry. In the scope of “Flexible, Fast and Future Factory” (F-3) project, work on 7 industrial sub-projects (case studies) and innovative manufacturing models were carried out to bring revolution in the chemical production industry of Europe. All seven case studies have directly or indirectly worked on developing a computer aided model to carry out smooth transition of batch to continuous production and the process intensification for high viscous polymers. Specifically, the case study 1st, 4th,5th, and 7th has demonstrated the feasibility of the transition to continuous production of acrylic acid [10]. There are several research papers that are either initiated or inspired by this €30 million funded project and some of them that are relevant to this thesis are discussed in this chapter. Below each of the papers is reviewed individually, followed by a brief synthesis of the existing literature.

2.1 Hashemi et al (2013)

Hashemi et al (2013) [18] designed a computer-aided model using Model Predictive Control (MPC) that is discretized by the Weight Essentially Non-Oscillatory (WENO) scheme to optimize productivity within the product quality constraints.

The study is based on experiments at 20% TS and uses multiple feed tubular reactor configuration. They also anticipated fouling using a mathematical tool named as “the bias correction” method, in which the deviation between the simulation results and experimental measurements is compensated by adding an error into the model for the next sampling time.

This paper also observed highest viscosity and maximum decrease in heat transmission (between the reactor and jacket) in the last segment of tubular reactor. This suggested more fouling in the last segment. The paper's observations were consistent with my thesis's idea to distribute the monomer concentration in a way- that the largest fraction goes in the first feed and the smallest in the last to avoid clogging as much as possible.

2.2 Micic et al (2014)

Micic et al [20] examined reactions with greater than 10% total solids (=17.7%TS; MW.= 23kg/mol) and successfully demonstrated a controlled radical polymerization process using Reversible Addition Fragmentation Chain transfer (RAFT) reagent to scale up a small laboratory process of 5ml scale by a factor of 100. To study the impact of the size and type of the reactor, an experiment was conducted in which the polymer product of a series of different reactors for batch and continuous process with different heating arrangements was compared. The initiator used was 4,4'-azobis (4-cyanovaleric acid), and a RAFT reagent was also used.

For the continuous process, a 500 ml scale-up RAFT polymerization was conducted in a prototype tubular flow reactor known as the Salamander flow reactor. The tubing was housed in a metal heating block, and a series of electrical cartridge heaters provided heating. The reactor was equipped with static mixers to enhance the mixing of the reagent solution.

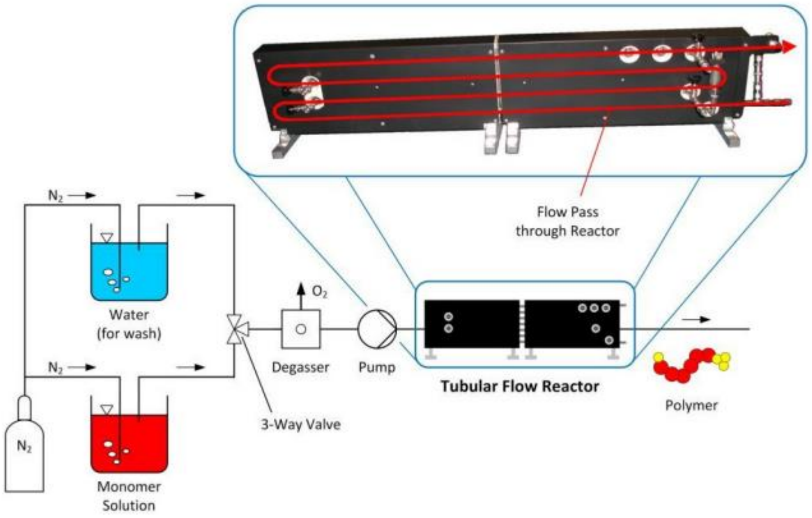

Figure 1 Flow diagram of the continuous tubular configuration for RAFT polymerization of water-soluble monomers

The paper observes that the larger batch reactor shows much more increase in the temperature profile than that of a smaller batch reactor due to a lower surface area-to-volume ratio. The same is true for batch reactors when compared with continuous tubular ones. In either case, the higher heat accumulation raises monomer conversion and reduces MW. Lower dispersity was noticed for batch than continuous, but no quantitative explanation was given. The paper has discussed the effect of temperature on polydispersity but has yet to explain it quantitatively. The paper was helpful for this thesis as the experimental results on a tubular reactor were based on a relatively higher monomer concentration (about 17% TS). This indicates that producing polymer at 17 %TS is possible using a tubular flow process. Although the paper has reported that the phenomenon of polymer clogging was happening inside the tubular wall at 17%TS; however, it does not explain which parameter is responsible for the deposition.

2.3 Qui et al (2016)

The paper studied the kinetics of acrylic acid polymerization in aqueous solution by using a microreactor [16]. The impact of flowrates, monomer concentration (2.5%TS to 10% TS), initiator concentration and reaction temperature (80-95 degrees celcius) on the monomer conversion were investigated. The molecular weight of 120-180 kg/mol was realized.

The microreactor consisted of five individual parts in a water bath. There was a mixing system to pre-heat and mix monomer and initiator solutions in water bath 1, two tubular arrangements used to adjust the reaction time inside the water bath 2 and 3, an additional tubular configuration to extend the reaction time in baths 4, and a quenching system to terminate the polymerization in bath 5 as shown in Figure 2.

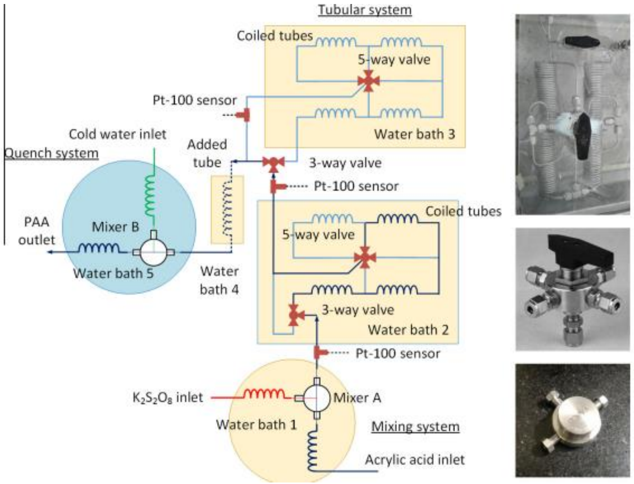

Figure 2 Schematic diagram of microreactor with picture of main elements.[1]

From the experimental results which were done with a 10%TS (low concentration), the paper concluded that with the increase in the initiator loading and temperature, the molecular weight decreases. It was also observed that the polydispersity increases with increase in temperature; however, no explanation was given.

The paper was successful in defining the expression of the kinetic equation of acrylic acid polymerization but has not considered the side chain reactions like backbiting. However, the defined

---

[1] Reprinted from Chemical Engineering Journal, Vol 284, Lu Qiu,Kai Wang,Shan Zhu,Yangcheng Lu,Guangsheng Luo, Kinetics study of acrylic acid polymerization with a microreactor platform, 233-239, 2022, with permission from Elsevier.

expression was not consistent with the model by Florit [11] and Illare et al [13] which published later in the year 2020. The paper is relevant to this thesis since I have used the analogous idea of using an ice bath to cool down the samples before collection from the quenching system used in the microreactor.

2.4 Chevrel et al (2016)

Chevrel et al (2016) [19] demonstrate a different way to establish a mathematical model using kinetics and rheological equations via a lab-scale continuous tubular reactor. This paper on the continuous pilot-scale tubular reactor for acrylic acid polymerization using a rheometer and Raman spectrometer data that demonstrates the concept. For designing a mathematical model, all kinetic parameters were determined by applying the Rheo-Raman experiments obtained in a lab-scale batch reactor. The model equations and the parameters from the Rheo-Raman device were used to get the overall mathematical model that was solved using MATLAB. The model-predicted values were then compared with the experimental values. For TS between 5 and 10 wt%), the weight-average molar mass was around 1000 kg/ mol. Eight tubular jacketed reactors of the Contiplant technology (Fluitec) were considered for the pilot-scale continuous reactor.

The paper only considered reactions at low monomer concentration, and the maximum total solids it studied is 10%. The increase in pressure drop with time for 10%TS could be because of polymer deposition inside the reactor. The paper is significant for my thesis because all the evaluations are based on the samples collected experimentally on the tubular configuration and not just on the predictive data estimated by the model. However, the TS% used in this paper is smaller than specified for this thesis. The paper also mentioned the fouling or deposit formation even at such a low TS%. It also concludes that there is a correlation between the viscosity of the reaction medium and deposit formation, but the correlation has yet to be investigated.

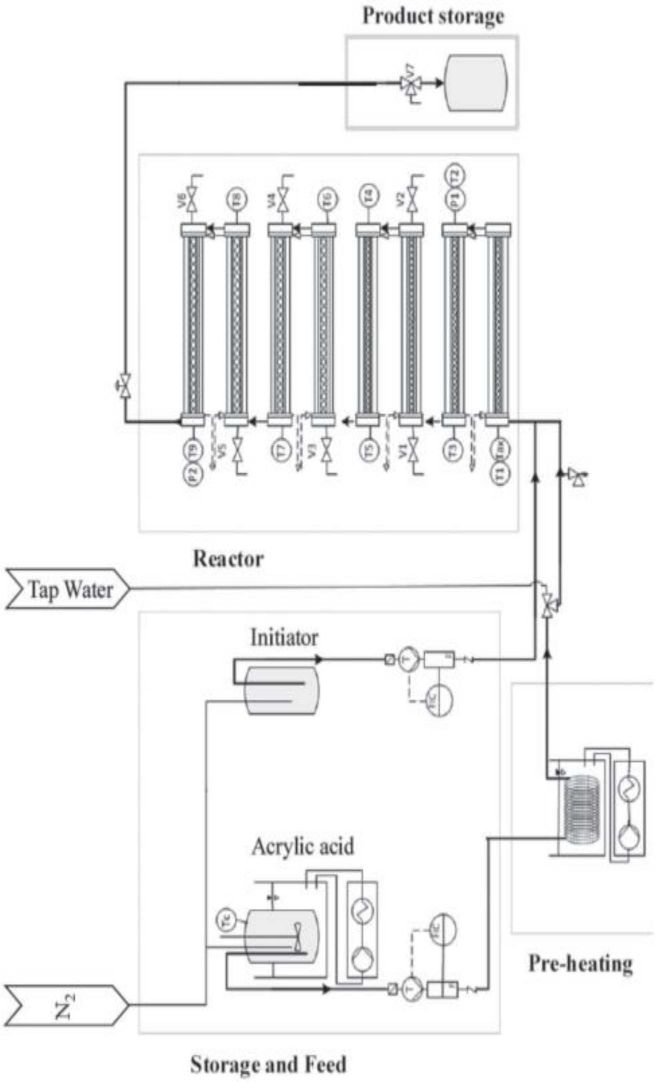

Figure 3 A schematic diagram of Pilot-scale tubular reactor.[2]

---

[2] Reprinted from Macromolecular Reaction Engineering, Vol 10, Alain Durand, Laurent Falk, Dimitrios Meimaroglou, et al, Continuous Pilot-Scale Tubular Reactor for Acrylic Acid Polymerization in Solution Designed Using Lab-Scale Rheo-Raman data, 10., 2022, with permission from John Wiley and Sons.

2.5 Brocken et al (2017)

Brocken et al [21] studied various conditions for the FRP of AA in a continuous flow arrangement. The reaction was carried out in a FlowSyn (Uniqsis Ltd., UK), as shown in Figure 4. This same system was used in the early part of this thesis. The maximum monomer concentration was restricted to 0.01% TS for the study, which was very low relative to other papers, to avoid clogging the reactor.

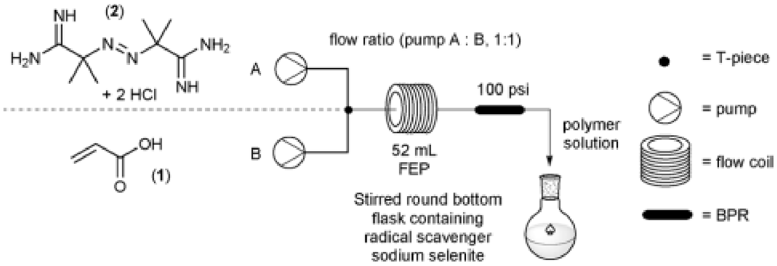

Figure 4 Flow scheme for the polymerization of acrylic acid.

It was observed that the molecular weight reduces at higher initiator loading, higher temperatures, lower monomer concentrations, and shorter residence time. High conversion could be reached at longer residence times. To obtain a good conversion at short residence times, elevated temperatures were required. Higher initiator is also observed to produce a lower average polymer chain and hence lower molecular weight. Even higher temperatures, lower monomer concentrations, and shorter residence time similarly reduce the polymer propagation and produce lower molecular weight. Another important takeaway from the paper was that temperature and residence time are the significant factors that increase monomer conversion and dispersity. This implies that narrowing down the dispersity and getting a good conversion simultaneously will be difficult. The paper has studied the effect of different operational conditions on product parameters. Still, it would be more interesting to see these results for a higher monomer content (or total solids).

This paper is relevant for this thesis because it showed work on the FlowSyn reactor, same as the early part of this research.

2.6 Florit et al (2020)

Florit et al (2020) developed a kinetic model using population balances via the method of moments (MoM) to convert the batch process to a continuous one based on a tubular reactor with intermediate feeds [11]. Their work aimed to develop a comprehensive chemical reaction model for the polymerization of undissociated acrylic acid (AA) in an aqueous solution using the couple sodium persulfate (PS)/sodium metabisulfate (MBS) as redox initiator.

For the kinetic scheme, the basic structure of the polymerization process (initiation, propagation, and termination), along with backbiting and transfer reactions to monomer/MBS, were taken into account since MBS is a chain transfer reagent. A complete set of involved reactions is given in Table 1 and the values of rate constants in Table 2 [22-24]. Buback et al [23, 26]measured most of the rate constant values. The article reported that the contribution of transfer reactions and backbiting was crucial for model predictions. Due to the use of transfer reagent MBS, transfer reactions to MBS are more effective in estimating the molecular weight distribution than transfer reactions to monomers. First, the model for SBR was developed and tested to validate the kinetics scheme using experimental data. Then the model for tubular reactors in series with intermediate feed streams was presented and applied to match the exact product specifications as that produced experimentally using an SBR.

As per this article, the tubular reactor should have multiple intermediate feeds for a model to match exact polymer specifications as given by an SBR experimentally. This idea was implemented in this thesis to reach the targeted specifications assigned by Lubrizol and to get stable operations without clogging. Also, the reaction kinetics provided in this paper was helpful in developing a clear understanding on analyzing experimental results of this thesis. To validate the kinetic model of the tubular reactor, the predicted model values were fitted to the SBR experimental data since no experiment runs were reported for the tubular reactor setup in this article. The total solids aimed in this work were low(=10%TS); hence, the article has not covered complications such as gel deposition on the tubular walls, which are more likely to occur at much higher TS% than 10%. Therefore, even in the model, no parameters were considered for polymer deposition inside the reactor.

Table 1 Reactions mechanism and their corresponding reaction rates [11].

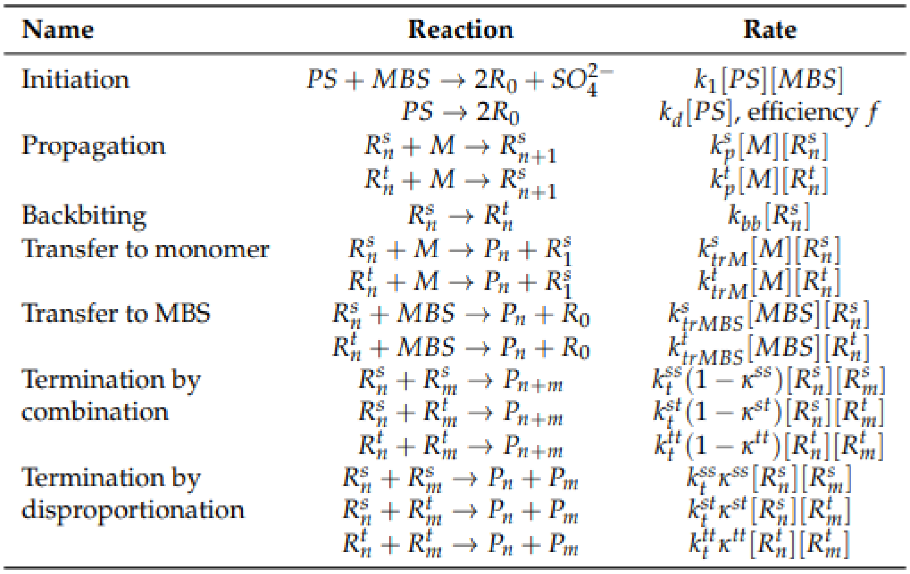

Name	Reaction	Rate
Initiation	$PS + MBS \rightarrow 2R_0 + SO_4^{2-}$	$k_1[PS][MBS]$
	$PS \rightarrow 2R_0$	$k_d[PS]$, efficiency f
Propagation	$R_n^s + M \rightarrow R_{n+1}^s$	$k_p^s[M][R_n^s]$
	$R_n^t + M \rightarrow R_{n+1}^s$	$k_p^t[M][R_n^t]$
Backbiting	$R_n^s \rightarrow R_n^t$	$k_{bb}[R_n^s]$
Transfer to monomer	$R_n^s + M \rightarrow P_n + R_1^s$	$k_{trM}^s[M][R_n^s]$
	$R_n^t + M \rightarrow P_n + R_1^s$	$k_{trM}^t[M][R_n^t]$
Transfer to MBS	$R_n^s + MBS \rightarrow P_n + R_0$	$k_{trMBS}^s[MBS][R_n^s]$
	$R_n^t + MBS \rightarrow P_n + R_0$	$k_{trMBS}^t[MBS][R_n^t]$
Termination by combination	$R_n^s + R_m^s \rightarrow P_{n+m}$	$k_t^{ss}(1-\kappa^{ss})[R_n^s][R_m^s]$
	$R_n^s + R_m^t \rightarrow P_{n+m}$	$k_t^{st}(1-\kappa^{st})[R_n^s][R_m^t]$
	$R_n^t + R_m^t \rightarrow P_{n+m}$	$k_t^{tt}(1-\kappa^{tt})[R_n^t][R_m^t]$
Termination by disproportionation	$R_n^s + R_m^s \rightarrow P_n + P_m$	$k_t^{ss}\kappa^{ss}[R_n^s][R_m^s]$
	$R_n^s + R_m^t \rightarrow P_n + P_m$	$k_t^{st}\kappa^{st}[R_n^s][R_m^t]$
	$R_n^t + R_m^t \rightarrow P_n + P_m$	$k_t^{tt}\kappa^{tt}[R_n^t][R_m^t]$

Table 2 Reaction rate constants (first order constants in [1/s] and second order in [1/mol.s]); Temperature in [K] [11].

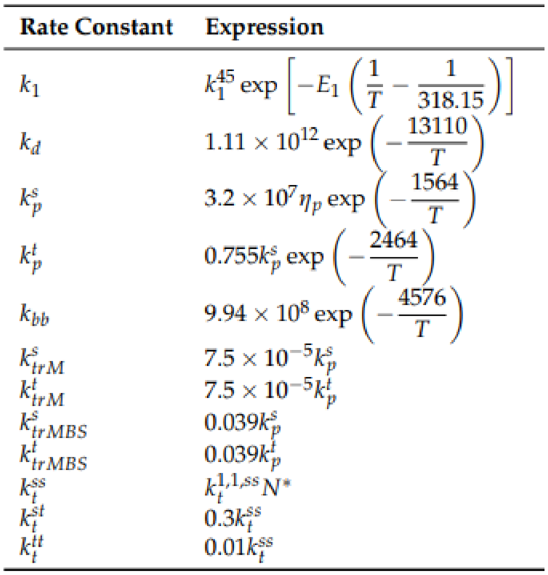

Rate Constant	Expression
k_1	$k_1^{45}\exp\left[-E_1\left(\frac{1}{T}-\frac{1}{318.15}\right)\right]$
k_d	$1.11\times10^{12}\exp\left(-\frac{13110}{T}\right)$
k_p^s	$3.2\times10^{7}\eta_p\exp\left(-\frac{1564}{T}\right)$
k_p^t	$0.755k_p^s\exp\left(-\frac{2464}{T}\right)$
k_{bb}	$9.94\times10^{8}\exp\left(-\frac{4576}{T}\right)$
k_{trM}^s	$7.5\times10^{-5}k_p^s$
k_{trM}^t	$7.5\times10^{-5}k_p^t$
k_{trMBS}^s	$0.039k_p^s$
k_{trMBS}^t	$0.039k_p^t$
k_t^{ss}	$k_t^{1,1,ss}N^*$
k_t^{st}	$0.3k_t^{ss}$
k_t^{tt}	$0.01k_t^{ss}$

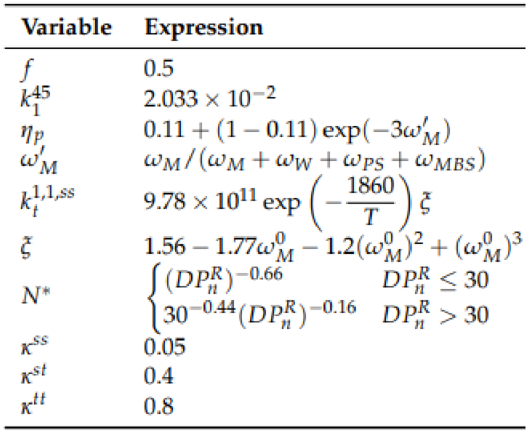

Variable	Expression
f	0.5
k_1^{45}	2.033×10^{-2}
η_p	$0.11+(1-0.11)\exp(-3\omega'_M)$
ω'_M	$\omega_M/(\omega_M+\omega_W+\omega_{PS}+\omega_{MBS})$
$k_t^{1,1,ss}$	$9.78\times10^{11}\exp\left(-\frac{1860}{T}\right)\xi$
ξ	$1.56-1.77\omega_M^0-1.2(\omega_M^0)^2+(\omega_M^0)^3$
N^*	$\begin{cases}(DP_n^R)^{-0.66} & DP_n^R\leq30\\30^{-0.44}(DP_n^R)^{-0.16} & DP_n^R>30\end{cases}$
κ^{ss}	0.05
κ^{st}	0.4
κ^{tt}	0.8

2.7 Illare et al (2020)

Similar to Florit et al, this paper [13] aims to develop a kinetic model and then validate it by comparing it with the experimental results from three reactor configurations: Batch, semi-batch, and continuous flow reactor. Brocken et al [21] studied various conditions for the FRP of AA in a continuous flow arrangement. The initiator used was aqueous solution of 2,2’-azobis (2- methylpropionamidine) dihydrochloride. For the initiator, they used an ammonium persulphate (APS) aqueous solution. The kinetic model of a tubular reactor with intermediate feeds was studied by Florit et al; however, this paper uses a continuous stirred tank reactor (CSTR). The model was first validated for batch and semi-batch configuration by using conversion and molecular weight data of the reactions for 5% and 21% TS at different temperatures ranging between 60 to 80˚C. After validating the model for the batch and semi-batch configuration, it was applied to a CSTR at a TS of 20%, compared against experimental results at steady state.

Further calculations were performed at higher TS. At TS= 35%, the predicted productivity (mass of polymer produced per unit time and reactor volume, g /ml/min) of a CSTR was much larger than that of an SBR. However, an increase in productivity also indicates a higher rate of polymerization and, hence, larger heat generation, which can be removed using cooling equipment. In fact, my thesis uses a tubular reactor instead of a CSTR since a tubular reactor has a high surface area to volume ratio for heat transfer. CSTR calculations were performed for 35% TS at a molecular weight of 400 kg/mol; however, no experiments were conducted under these conditions. An increase in the polymer deposition rate is expected for such a high total solid and molecular weight but it was not discussed.

2.8 Summary of Literature on continuous production of PAA

The literature review provides adequate information on the kinetic scheme of free radical polymerization of acrylic acid using an aqueous solution of persulfates as initiators. The kinetic schemes helped interpret the experimental results and correlation between parameters achieved in the thesis work. Most of the reviewed papers in the chapter were computational, with limited information on the experimental validation of those computational models. For FRP of PAA, past research papers have investigated reaction kinetics at lower monomer concentration than targeted in this thesis (the maximum reported total solids was 17% by Micic et al [20], whereas most are at or below 10% monomer). Many have predicted results at high monomer concentrations computationally, for instance-work by Illare et al [13] and Hashemi et al [18], without experimental validation. The investigation of continuous production at high monomer content (about 25%) of acrylic acid, the crucial aspect of this thesis, has yet to be discussed in the literature. The experimental data at lower solids loading have clearly documented the effect of temperature and residence time on conversion and molecular weight. Some papers (like by Qiu et al [16] , Micic et al [20], and Chevrel et al [19]) have also mentioned the dependence of polydispersity on temperature, although without mechanistic explanation. Perhaps most importantly, reactor fouling due to the deposition of the polymer in a continuous reactor over time, and thermal runaway, have yet to be discussed, whereas these parameters are crucial to any commercial continuous manufacturing operation. Some of the reviewed computational research papers did not have much information on polymer deposition inside the reactor except for one - the kinetic model by Hashemi et al. It has established the controller-based computational model which uses the biased correction method that acknowledges and addresses fouling.

This thesis aims to produce PAA using continuous processes at total solids (25%), which far exceeds the experimental literature. We anticipate that this will pose challenges such as high rate of polymer deposition in the reactor, resulting inconsistency in the product properties, and possibly thermal runaway. This thesis work was able to develop a robust process configuration that can efficiently address these issues.

3.0 Experimental Setup

3.1 Materials

The experimental tests were run using acrylic acid (99% pure with 200ppm MEHQ- monomethyl ether hydroquinone as an inhibitor), ammonium persulfate, and phenothiazine (shortstop). All the chemicals were purchased from Fisher Scientific or from Sigma-Aldrich and sometimes from Lubrizol. The sodium selenite was purchased from Alfa Aesar and is kept nearby as an emergency radical terminator. The chemicals were used as received without further purification. The flow polymerization was originally carried out on a FlowSyn (Uniqsis Ltd., United Kingdom). Then the configuration was switched to a two-feed-monomer setup and the experiments were continued on the Lubrizol setup consisting of three Eldex pumps (two of them for the monomer feed and one for the initiator) and a coiled tubular reactor inside a hot glycol bath.

3.2 The FlowSyn Instrument and the Tubular Reactor

The main goals of the thesis were 1) to safely transit from batch to continuous flow production of high monomer content PAA; 2) to produce PAA product using continuous flow that is of equivalent specs as such as 300,000 g/mol molecular weight, a polydispersity of 10 or below, and a PAA concentration of 25% with 99% conversion, and 3) to establish a thermally stable reaction that can produce PAA for long durations. The research was originally conducted on the FlowSyn instrument (Uniqsis Ltd.) as shown in Figure 5. Several research papers have demonstrated FlowSyn's capabilities for continuous FRP, such as the paper by Brocken et al [21], which is also reviewed in the Literature Review section of the thesis, explicitly reports FRP of AA at low monomer concentrations. The FlowSyn instrument used for the thesis has two continuous HPLC (High Performance Liquid Chromatography) pumps (each capacity of 50 mL) with a pre-installed 2.8 bar back pressure regulator (BPR). The instrument has a 2 ml glass chip mixer, to ensure thorough mixing of the reactants before reaction, and an internal pressure reading arrangement. An additional pressure sensor (Vernier) is placed before the hot bath, to gauge variations in the viscosity of the product. The pressure sensor is set up to collect data every 3 seconds and produces a real-time graph of the pressure of the system. Since the thesis aimed to produce polymer at higher total solids, it was susceptible to polymer plugging issues, and cleaning the clogged coiled stainless-steel tubing is itself a challenge. To address the plugging issues, the inbuilt stainless-steel coil in the instrument was replaced with a PTFE tubing (1/8″- ID and 3/16″ OD purchased from McMaster- Carr) coiled in the hot water bath, which is a Pyrex trough (Corning) with a magnetic stirrer to prevent the formation of hotspots, placed over a hotplate (Thermo Scientific) with an attached thermocouple. The intention to resort to PTFE tubing was- 1) to replace the tubing whenever the permanent plugging occurs and 2) to observe the flow through the translucent PTFE material. After the reaction in the coiled tubing inside the hot bath, the product was collected in 60 ml HDPE bottles (Fisher Scientific) and then sent for further analysis and characterization.

.

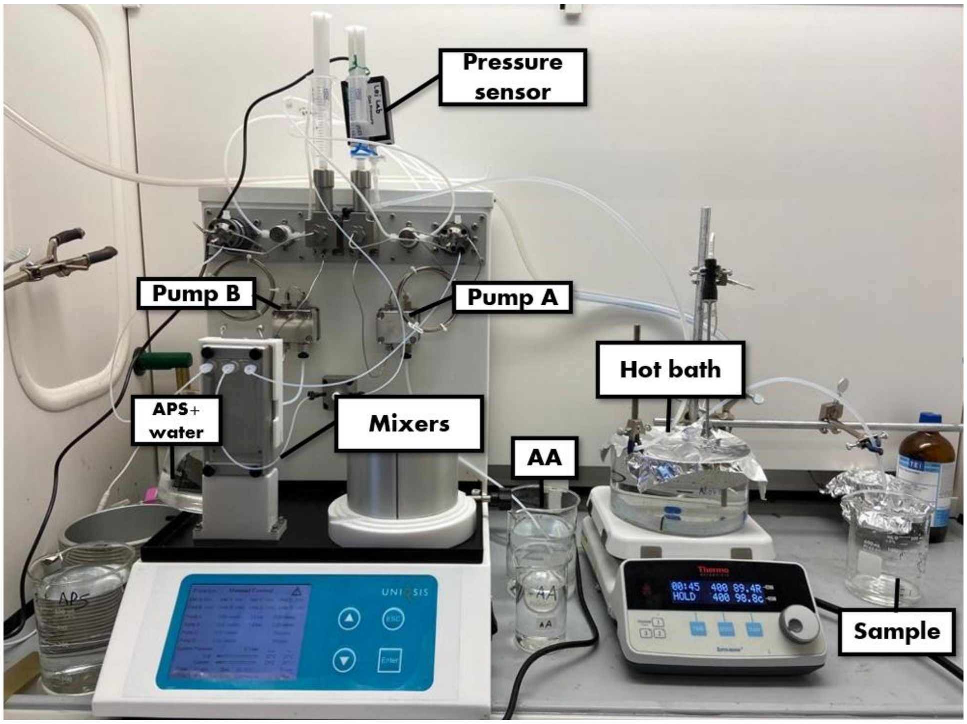

Figure 5 The tubular configuration consists of the FlowSyn instrument, a pressure sensor, and a hot bath over a hot plate where the reaction takes place (Pitt Lab).

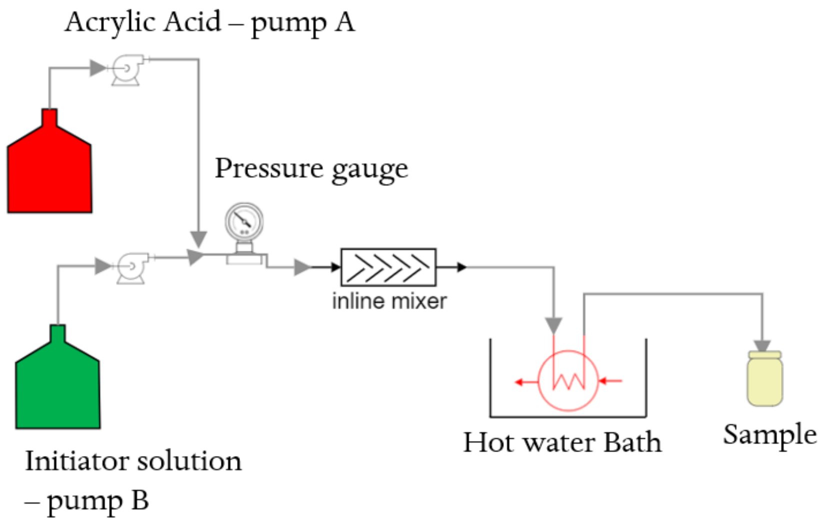

Figure 6 Schematic diagram of the FlowSyn reactor configuration

3.3 The Tubular Reactor Configuration with Two Monomer Feed

The clogging in FRP is the most frequent due to difficulty in solubilization at high concentrations and the increasing viscosity with time. Moreover, the sticky nature of the polymer also aggravates the polymer deposition inside the reactor, restricting the flow. This also impacts the residence time and the heat removal capacity, affecting the process reproducibility (Ilare et al [13]). The issue of clogging at a high monomer content was addressed by an improved setup (as shown in Figure 7) used for the thesis, which is a two-monomer-feed tubular reactor configuration with two pumps to feed the monomer and one pump for the initiator solution. In other words, it is a tubular reactor with multiple monomer feeds. Hence, the idea behind switching to this configuration was to avoid any location in the reactor with a high monomer concentration so the system could avoid clogging effectively.

Figure 7 The tubular reactor configuration with two monomer feed (Lubrizol setup).

The monomer and aqueous solution of the initiator were first prepared for the reaction by deoxygenating the solution using nitrogen purging in the stainless-steel degasser feed tank. A BPR set at 20 psi was connected to the degasser. Then the stock solutions were pumped with Masterflex - Eldex piston pumps. An inline pressure gauge (psi) instrument was placed just before the feed point to monitor the system's pressure. The fed reactants were mixed through an inline static mixer (21 blades, 0.132” ID, stainless steel, McMaster-Carr) and then passed to the 25 ft long coiled Teflon tubing arrangement inside the hot glycol bath (at 90 C) as shown in Figure 8a., where the polymerization occurs. The reaction temperature of the glycol bath was controlled using a VWR heat/circulator. The outlet stream from the hot bath was mixed again with the second monomer feed via an inline static mixer and made to react the same way as earlier in the 25 ft long Teflon tubing in the coiled arrangement inside the hot bath. Five thermocouples were placed to monitor the temperature of the stream at five different locations- 1) the inlet stream before reaction; 2) the stream inside the bath where polymerization occurs; 3) the outlet stream coming out of the hot bath after the reaction of the first monomer feed; 4) the outlet stream coming out of the hot bath after reaction of the second monomer feed, and 5) the product. The temperature readings for all five locations were recorded using the MadgeTech banded temperature data loggers with the LCD screen (TCTempXLCD) as shown in Figure 8b.

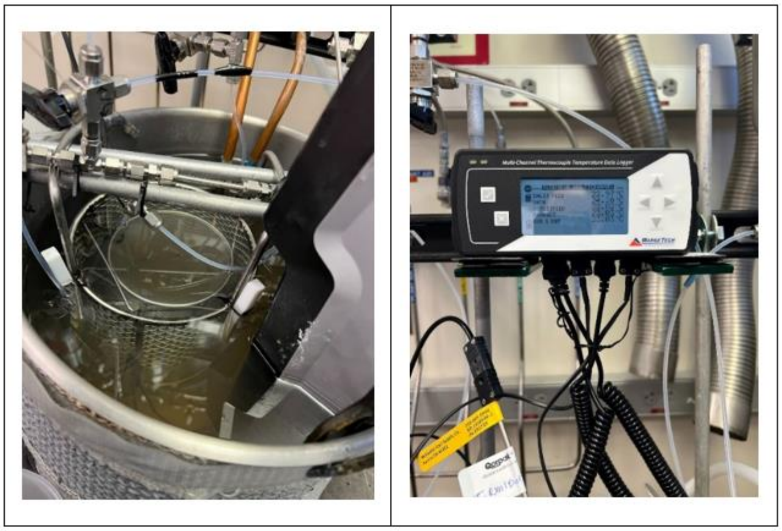

Figure 8 a. The Teflon tubing in coiled arrangement inside the hot Glycol bath (the reaction medium); b. The thermocouples are placed to monitor temperatures of the stream at various locations and these temperatures are recorded using the MadgeTech TCTempXLCD.

3.4 Sample Characterization

Lubrizol has conducted all characterizations in this research. Gel permeation chromatography (GPC) is used to determine the molecular weights and the polydispersity index (PDI) of the samples using the Waters 515 pump with 717plus auto-sampler and 2414 RI (Random Indexing) Detector at 40°C. The high-performance liquid chromatography (HPLC) is used to determine the residual acrylic acid (RAA) using a Phenom Luna 18 column with a run-time of 30 mins. The total solids (TS)% is determined by microwaving a few drops of the sample on a glass fiber pad and heating it dry. The in-built software in the microwave instrument set at 30% power for 10 secs determines the value based on the weight difference before and after moisture loss.

4.0 Results and Discussions

Several factors are considered to strategize the approach toward producing a product from a highly exothermic FRP reaction. One of the parameters is the adiabatic temperature rise that calculates the potential severity of a given reaction if cooling fails or if the rate of heat generation in a reactor exceeds that of the heat removal. From the safety perspective, estimating the adiabatic temperature rise is a helpful reactor design parameter to prevent runaway reaction scenarios and establish the ideal reaction procedure. If the concentration of unreacted monomer accumulates, it is hazardous if cooling fails. Highly exothermic reactions with a high adiabatic temperature can lead to a high reactor temperature. The undesired rise in the reactor temperature can evaporate all the solvent, increasing pressure in the reactor. The increased pressure of the system may restrict the flow of the reaction medium, causing polymer accumulation inside the tubing and, hence, thermal runaway. The adiabatic temperature rise can be estimated using the following equation:

$$\Delta T_{AD} = \frac{\{AA\}(\Delta H)}{c_p . \rho} \tag{4-1}$$

Where, {AA} is the acrylic acid concentration; ΔH is enthalpy of the reaction (63kJmol^{-1}); c_p is the specific heat capacity; ρ is the density of the reaction medium. Using the above equation, a ΔT_{AD} Vs. monomer concentration graph was plotted.

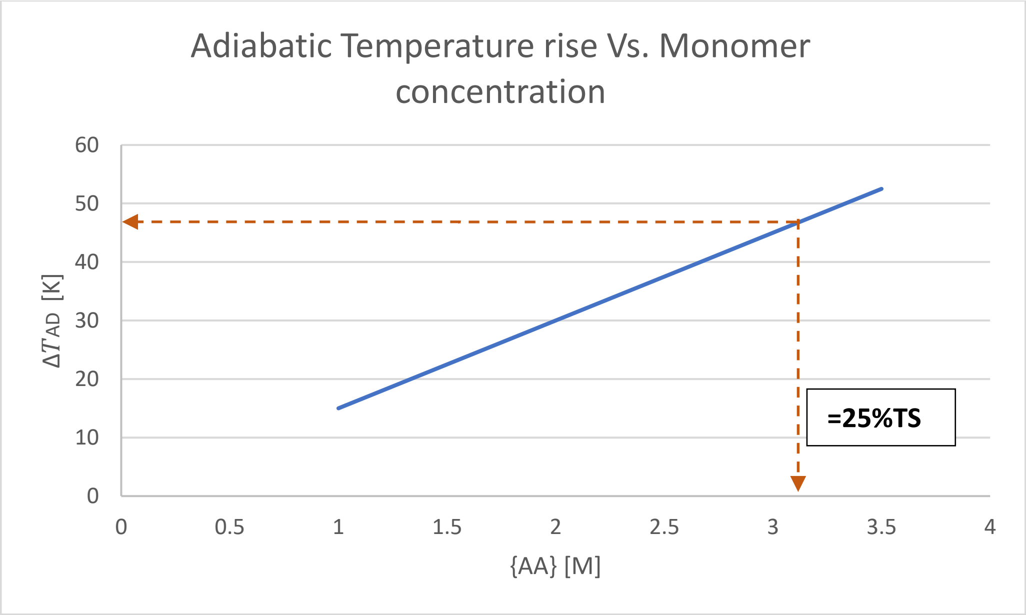

Figure 9 The adiabatic temperature-rise Vs. monomer concentration plot.

The monomer concentration used in the plot was in the range of 1 to 3.5M since most experiments were done within this range. The adiabatic temperature rises in the Figure 9 is already above the boiling point of the solvent which is 100^0 C. To prevent the rise in the temperature of the reactor or thermal runaway due to ΔT_{AD}, some measures were taken, such as the residence time was always kept small, the inline static mixers were implemented into the streamline and the monomer-initiator aqueous solution ratio was always kept below unity.

Several experiments with varying reaction conditions were conducted on the FlowSyn setup shown in the Figure 5 to study the system capabilities and reaction dynamics for which many factors are examined beforehand. The experiments were started with the aim of establishing stable reactions starting with the lower total solids PAA using different set of conditions. Since the polymerization at higher total solids is susceptible to polymer clogging, with the help of the real time pressure graphs, the maximum total solids % that delivers a stable reaction was determined. Starting at 5% TS, experiments with varying total solids at 90^0 C were carried out for the investigation. For all reactions, the pressure vs. time profiles showed a stable pressure line along with time and no random fluctuations until it reached 14% TS. The experiment run at 14% TS, or higher produces random fluctuations in the pressure graph, indicating polymer deposition inside the reactor. Sometimes high viscous polymer blobs in the polymer outflow were noticed at these fluctuations in the pressure graph. From this observation, all the future experiments for the FlowSyn setup were restricted to 13%TS. It could be due to high viscosity at low temperatures that the kinetics become diffusion limited and, hence, resulting in the increased probability of the gel effect. Any disturbance in the reaction dynamics, like the gel effect or high viscous blobs of polymer in the stream, will be noticed by the vernier pressure graph placed on the FlowSyn setup. Hence, it was observed from the pressure graph (Figure 25) that the fluctuations in the pressure line reduce with increasing temperature. Therefore, for temperatures above 85^0 C, the system produces more stable operation.

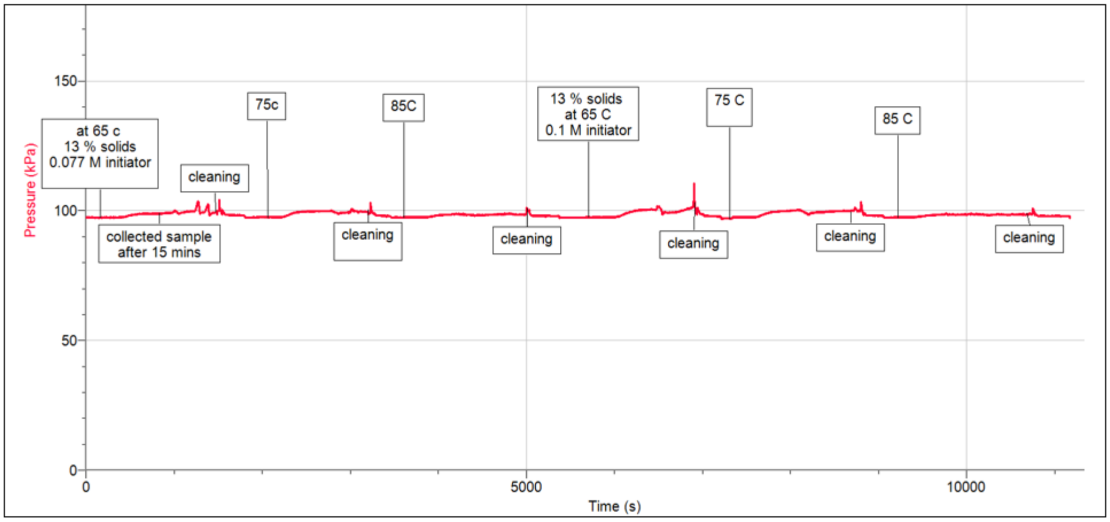

Figure 10. The vernier pressure vs time graph of an experiment ran at 13%TS; At three different temperatures: [65,75,85]^{0}C and two different initiator loading [0.077,0.1] M on the FlowSyn reactor setup at University of Pittsburgh Lab.

From the Table 3 polymer properties, the experiment's result agrees with the conclusion made by Brocken at El [21]. The paper states that the temperature, RT, and initiator loading are the major factors that impact the conversion. At fixed residence time, the conversion was found to increase with increasing temperature. With the increase in the initiator loading, the conversion rises significantly. However, with increasing initiator concentration, the molecular weight reduced, and the PDI increased. With the increase in the initiator concentration for fixed monomer concentration, there will be an increase in the initiating radicals and, therefore, in the multiple competing polymerization events, shorter polymers will be formed as the monomer concentration will not be enough to produce long chains. This can also be explained by the empirical equations of rate of initiation, R_I, and rate of propagation, R_p, and number-average degree of polymerization is given.

$$R_I = k_d.f.\{I\} \tag{4-2}$$

$$R_p = \{M\}k_p\sqrt{\frac{k_d.f.\{I\}}{k_t}} \tag{4-3}$$

$$X_n = \frac{R_P}{R_I} \tag{4-4}$$

$$X_n = \frac{\{M\}k_p}{\sqrt{k_d.f.\{I\}.k_t}} \tag{4-5}$$

According to Equation 4-5, the degree of polymerization is inversely proportional to the square root of the initiator concentration. The degree of polymerization is directly proportional to the kinetic chain length, υ, or sometimes equal (in the case of disproportionation termination). It implies that with the increase in the initiator concentration, the polymer chain length will decrease. Also, from equation 4-6, where M_w^0 is the molecular weight of the monomer, it can be inferred that the molecular weight of the polymer decreases with the increase in the initiator. Also, the increase in the molecular weight is expected with the increase in the molecular weight as both are directly proportional to each other.

$$M_n = X_n.M_w^0 \tag{4-6}$$

Below is the degree of polymerization vs. initiator concentration graph at three temperatures = [65, 75, 85]^0 C. From the graph, it is observed that the experimental values of initiator concentration at temperature 85^0 and 75^0 C are showing somewhat similar trend to that of the calculated values (using Equation 4-5). However, the slope for the initiator concentration values at temperature 65^0 C seems completely off as compared to that of the calculated ones. It could be an indication of polymer deposition inside the tubing, which could also be interfering with the polymer properties.

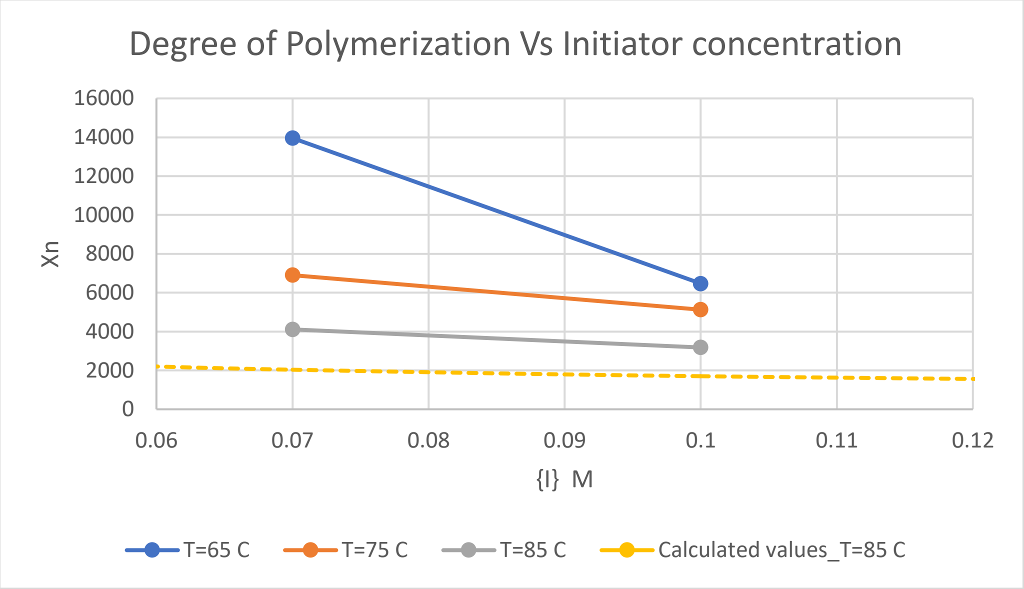

Figure 11 Number-average Degree of Polymerization with respect to temperature at two initiator concentration- [0.07, 0.1] M; using Equation 4-10.

A similar effect on molecular weight due to the temperature rises can also be ascribed to the increase in the formation of initiating radicals. This can be explicitly explained by plotting the degree of polymerization against temperatures by using Equation 4-10. This equation is derived by taking the logarithm of Equation 4-5 and then expanding the reaction constants in the form of Arrhenius equations. The values of the pre-exponential coefficient and the activation energy for initiation, propagation and termination reactions are taken from the reviewed literature and are given in Equations 4-7 to 4-9. It is worth noting that the activation energies ($E_p - \frac{E_d}{2} - \frac{E_t}{2}$) given in Equation 4-10 for the degree of polymerization (X_n) is a positive value, which implies that the X_n is decreasing with increasing temperature. The X_n values reduced by 80.69% when the temperature increased from 65^0 to 85^0 C.

$$k_d = 1.17 \times 10^{22}. exp\left(\frac{-21169}{T}\right) \qquad 4\text{-}7$$

$$k_p = 3.2 \times 0.712 \times 10^{7}. exp\left(\frac{-1564}{T}\right) \qquad 4\text{-}8$$

$$k_t = 9.78 \times 1.3299 \times 10^{11}.\,exp\left(\frac{-1860}{T}\right) \tag{4-9}$$

$$\ln X_n = \ln\frac{A_p}{(A_d A_t)^{1/2}} + \ln\frac{\{M\}}{f.\{I\}^{1/2}} - \left(\frac{E_p - \frac{E_d}{2} - \frac{E_t}{2}}{RT}\right) \tag{4-10}$$

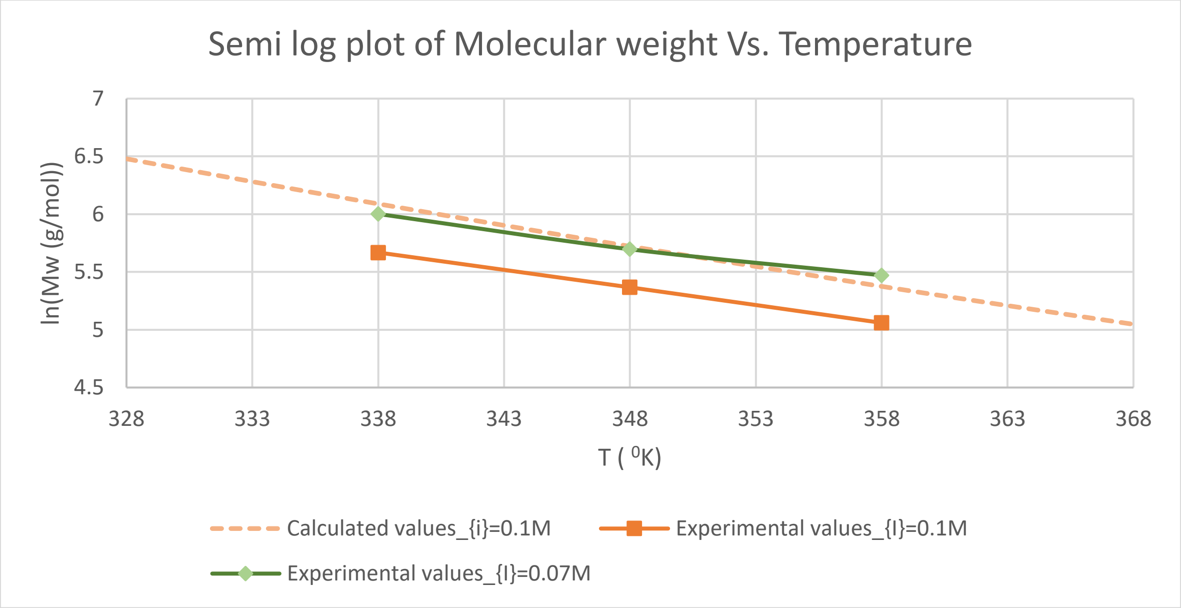

Figure 12 Semi-log plot of number-average molecular weight with respect to temperature using calculated values from Equation 4-10 and experimental values from the table 6 (at {I}=0.1M)

Similarly, a semi-log graph of number average molecular weight is plotted using the calculated X_n values (Equation 4-6) and is compared with the experimental molecular weight values from the Table 3. The graph clearly demonstrates the decrease in molecular weight values with increasing temperature. Here, it can also be observed that the trend at {I}= 0.07M is a little off as compared to that of the calculated values (using Equation 4-10). It was due to large molecular weight values at 65^0 C temperature which could also indicate presence of high viscous blobs in the stream. Overall, the graph of the number average degree of polymerization with respect to the temperature demonstrates that with the increase in reactor temperature, the polymer chain length decreases, causing the molecular weight of the polymer to decrease. However, this increase in the temperature has caused the PDI to significantly increase. It can be due to more no. of radicals being in the picture, probably originating from more diverse polymer chains.

Table 3. The impact of temperature and initiator concentration on the Molecular weight and RAA values of the PAA at 13%TS.

SN	**T (^{0}C)**	**Molecular Weight (Kg/mol)**		**Residual Acrylic Acid (ppm)**		**Conversion (%)**		**Dispersity Index**	
		[I]= 0.077 M	**[I]= 0.1M**	**[I]= 0.077M**	**[I]= 0.1M**	**[I]= 0.077M**	**[I]= 0.1M**	**[I]= 0.077M**	**[I]= 0.1M**
A	65	1005	466	10596	1759	91.24	98.76	4.35	4.64
B	75	497	369	10518	1624	91.62	98.90	4.65	5.31
C	85	296	229	4372	1611	96.82	98.93	7.71	9.12

From the experiments on the tubular reactor shown in Figure 5 , much information was gathered about the reaction kinetics and the uncertainties, like fouling and the random fluctuations in the pressure graphs, that took place during polymerization. These random fluctuations in the graph were more frequent for the reactions with high monomer concentrations than the lower ones. Generally, increasing the monomer concentration in the FRP increases the rate of polymerization, causing an increase in the heat generation during the exothermic reaction, which was evident while collecting the visibly boiling sample (as shown in the Figure 13a.) for an experiment with a monomer concentration of 3M (24% TS).

Figure 13 a. The PAA product is still boiling even after collection; b. The chunks of highly viscous gel like matter in the outlet stream; c. The highly viscous chunk-blob stuck at the bottom of the sample bottle.

Ideally, for a system to effectively control the reaction thermally, the polymerization should have terminated as soon as the stream has left the reactor. However, the Figure 13a. depicts that the polymer in the sample bottle was still boiling, indicating that the polymerization may still be ongoing, and the reaction was not yet terminated. The residual acrylic acid (RAA) values from an experiment of the two different sample-collecting arrangements were considered to evaluate the deviation a thermally uncontrolled reaction could cause to the product characterization. These two arrangements were: 1) The polymer sample was collected in a bottle without cooling and without a shortstop; 2) The sample was collected in a bottle and kept in an ice bath with a shortstop. The experiment was conducted at two different RT and the RAA values at both residence times showed substantially lower values for the first arrangement than for the second one as shown in the Table 4. This confirms that the reaction continued after the polymer exited the heated section of the tubular reactor.

Table 4 The RAA values of the polymer samples collected in two different arrangements; the monomer and initiator concentration used were 3M and 0.068M respectively; The experiment was conducted for two residence time 1)1 min, 2)1.5min and at 90^0 C temperature.

SNo.	Residence Time(min)	Type of Sample collecting arrangement	Residual Acrylic Acid(ppm)
D1.	1	The polymer sample collected in a bottle without cooling and without a shortstop	80.44
		The sample was collected in a bottle and kept in an ice bath with a shortstop	1958
D2.	1.5	The polymer sample collected in a bottle without cooling and without a shortstop	78
		The sample was collected in a bottle and kept in an ice bath with a shortstop	1929

With reference to the considerable difference between the RAA values of both arrangements given in Table 4, it was decided to opt for the second arrangement for collecting samples as it was evidently better at terminating the continuing polymerization and significantly preventing the thermally uncontrolled reactions after exiting the reactor. Due to the unpredictable episodes of fouling and random trends in the product specifications for higher monomer concentrations(>13%TS), it was decided that the FlowSyn system was inefficient in producing polymer with higher total solids.

A more robust configuration was needed to replace the FlowSyn setup that effectively addresses the clogging issue. The tubular reactor with intermediate feeds was considered, starting with the two monomer feeds, as shown in Figure 7. That way, the monomer feed reacts in two fractions, rather than making the whole monomer feed react at once. This also implies that the monomer stream will now be reacted in two fractions, potentially lowering the probability of polymer clogging as the monomer concentration gets reduced; hence, the system can effectively prevent polymer deposition.

Before proceeding, it was necessary to decide whether the reactor should have a second initiator feed or not. So, an experiment was conducted to check how long the initiator solution continues to produce free radicals without decaying. The experiment consisted of six vials that had samples of aqueous initiator solution. These six samples were heated at 90^0 C for different depletion times: [0,1,2,3,4,15] mins and monomer (21%TS) was added to each as shown in the Figure 14. Upon heating to 90^0 C, all six pre-heated initiator solutions could react with the monomer. This suggests that all six pre-heated samples still had undecomposed initiator solution even after 15mins of depletion time. This agrees with the half-time of the initiator which is 50 mins at 90^0 C (calculated using the decay rate constant from the literature 21]). Therefore, it was decided not to include a second initiator feed into the tubular reactor because all the experiments were at residence time at not more than 4 mins which was lower than the calculated decay time of the initiator.

Figure 14 a. The vial containing initiator solution is kept in a hot bath at 90^0 C to heat for different depletion time: b. The vial after 15 mins when reacted with the monomer got all gelled up inside.

While experimenting with varying total solids [at 2.5 min RT; {I}=0.25 M; T=90^0 C] on the tubular reactor with two monomer feed, two observations were made: 1) The experiment operated at TS under 18% had random fluctuations in the pressure graph and frequently producing highly viscous blobs in the outlet stream; 2) The experiments operated at total solids above 18% failed after one hour of reacting time as the reactor gets clogged. Both observations indicated that the configuration was still not efficient in producing polymer for higher total solids and needs process improvisation. To address the issue, an experiment was conducted [at 2.5 min RT; 24%TS; {I}=0.20 M; T=90^0 C] where the pressure vs. time graph was monitored and compared for the two configurations (Figure 17). These configurations were: 1) The original tubular reactor with two monomer feeds; 2) The same tubular reactor with an additional feature of an ice bath implemented to cool off the product stream coming out of the first reactor before mixing it with the second monomer feed as shown in the Figure 15.

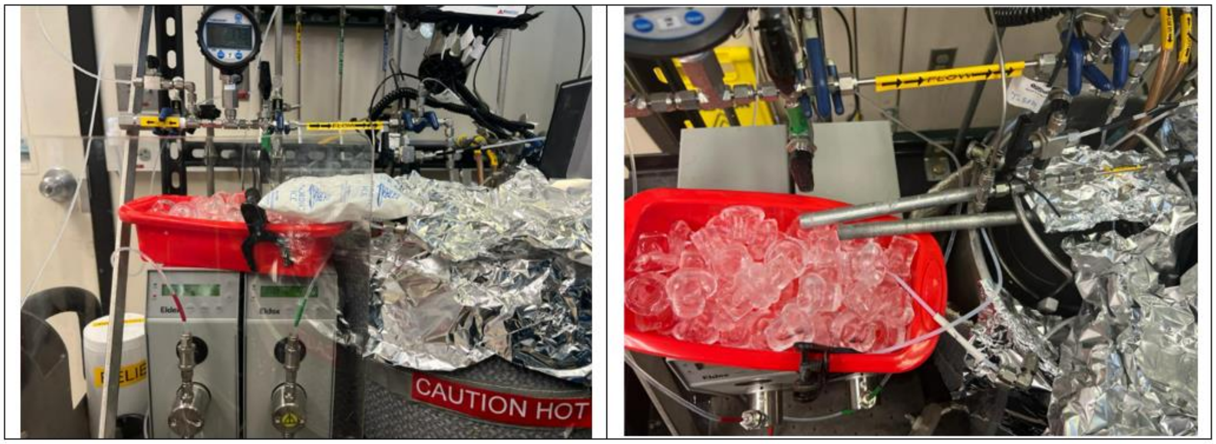

Figure 15 To cope up with the excess heat generated during polymerization, an ice bath was added to cool off the product stream coming out of the first reactor before mixing it with the second monomer feed.

Comparing the pressure vs time graphs, as shown in Figure 17, for the reaction with and without the ice bath, it was clear that adding an ice bath makes the reaction more stable. From the graph, the pressure seems more stable with time for the reactor with the ice bath, and whenever the ice bath is removed, the peaks and irregularities in the pressure line are observed. The observation indicates that the high temperature of outlet stream of the first reactor makes the second monomer feed react immediately upon being fed into the aqueous stream while it is still not thoroughly mixed with the aqueous stream. Thus, there may be regions very close to the inlet of the second feed which have a local concentration that far exceeds the average. This may cause the gel effect due to diffusion limitation. Due to diffusion limitations, the gel effect restricts the diffusion of growing polymer chains but not the diffusion of monomer molecules. Hence, the rate of termination reaction gets decreased (Trommsdorff effect) which needs two growing chain ends to collide, whereas the propagation rate constant stays the same, and the polymer chains keep growing. This phenomenon can be prevented if the solution is mixed thoroughly before passing it through the second heated segment of the reactor. Implementing an ice bath to cool the output of the first reactor before the second monomer feed slows down the reaction significantly. The subsequent static mixer just before the second reactor reduces the chances of the gelation effect and helps to produce a uniform polymer product with a lower polydispersity index. The peak in the pressure graph could be the result of flow restriction due to polymer deposition inside the reactor. The observation also implies that the outflow stream from the first reactor must be cooled before the second monomer feed gets added to the stream.

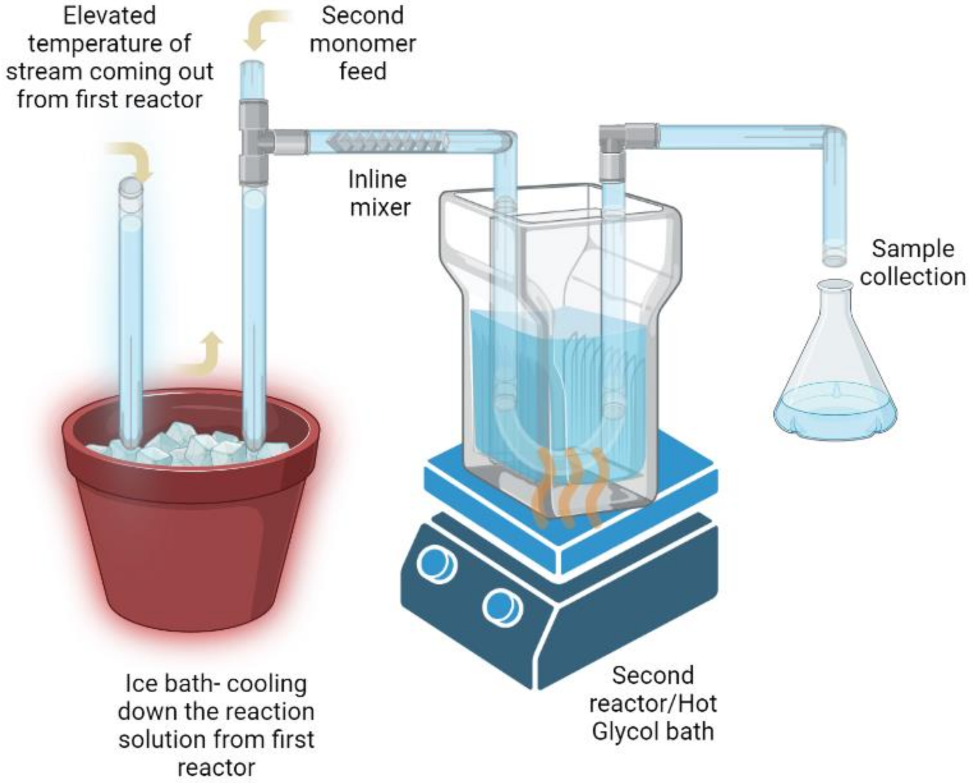

Figure 16 Diagram showing the location where the ice bath is installed in the two-monomer feed configuration.

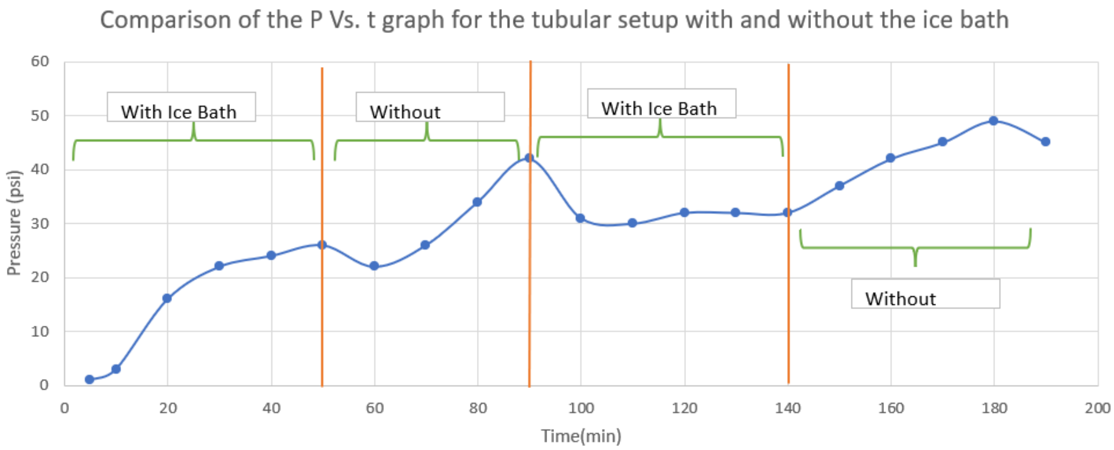

Figure 17. Comparison of the pressure Vs. time graph of the tubular setup with and without the ice bath at Lubrizol setup

It was decided to conduct more experiments to study the new setup with the ice bath. A schematic diagram of the final setup is given in the Figure 18.

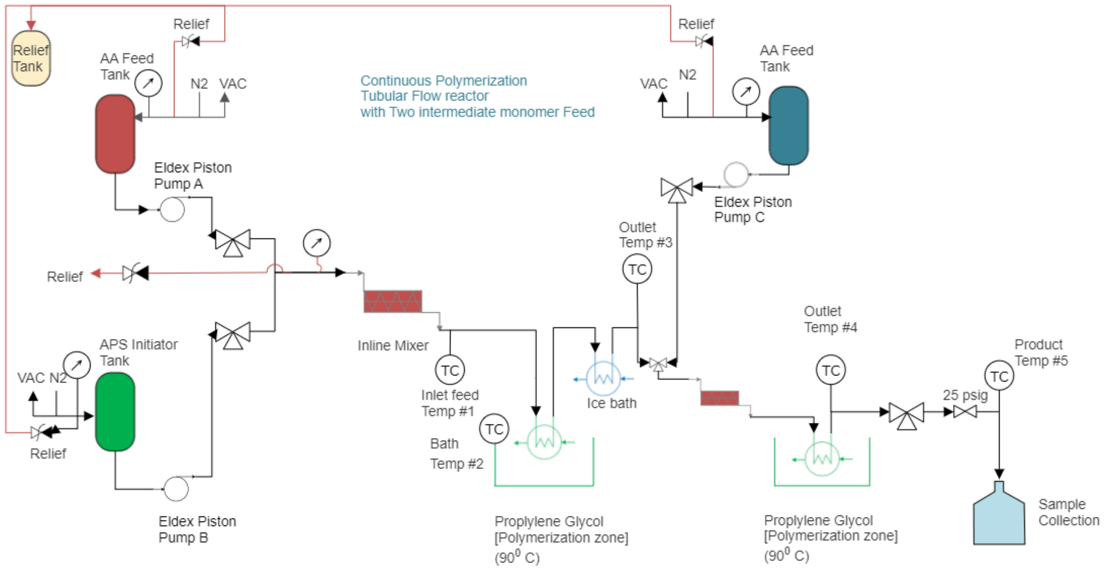

Figure 18 The schematic diagram of the final setup.

A set of experiments with the same monomer and initiator concentrations and conditions with and without the addition of an ice bath was conducted. The pressure vs. time graphs of all the experiments given in Table 5 were plotted and then compared. The table also states which experiments were successful and did not end up clogging the system. The successful experiments were referred to as 'S' and the experiments that got clogged were referred to as 'F' (=Failed).

Table 5. The set of experiments that were conducted before and after the addition of the ice bath to the reactor.

Run	RT (each reactor)	Total Solids%	Initiator Wt.	Temperature	Failed(F) or Successful (S)
1	2.5 min	25	0.2M	90 C	F
1a	2.5 min	25	0.2M	90 C	F
1b	2.5 min	25	0.2M	90 C	F
After adding the ice bath					
2	2.5 min	26	0.25M	90 C	S
3	2.5 min	25	0.2M	90 C	S
4	2.5 min	24	0.15M	90 C	S
5	2.5 min	24	0.1M	90 C	S
6	2.5 min	24	0.2M	90 C	S

The graphs in the Figure 19 clearly show that the pressure rose without becoming stable for Run 1, 1a, and 1b, indicating thermal runaway or polymer deposition inside tubing walls. Whereas, for Runs 2 to 5, the pressure line increased only in the first 20 mins of the reaction and stayed constant for the rest of the reaction time. The impact of adding an ice bath prior to the second monomer feed can be observed by comparing Run 1b and Run 3 as both experiments have the same concentrations and conditions. Before adding the ice bath, the experiments failed after 1 or 1.5 hours of work, but with the ice bath feature, experiments could work long as 4 to 5 hours.

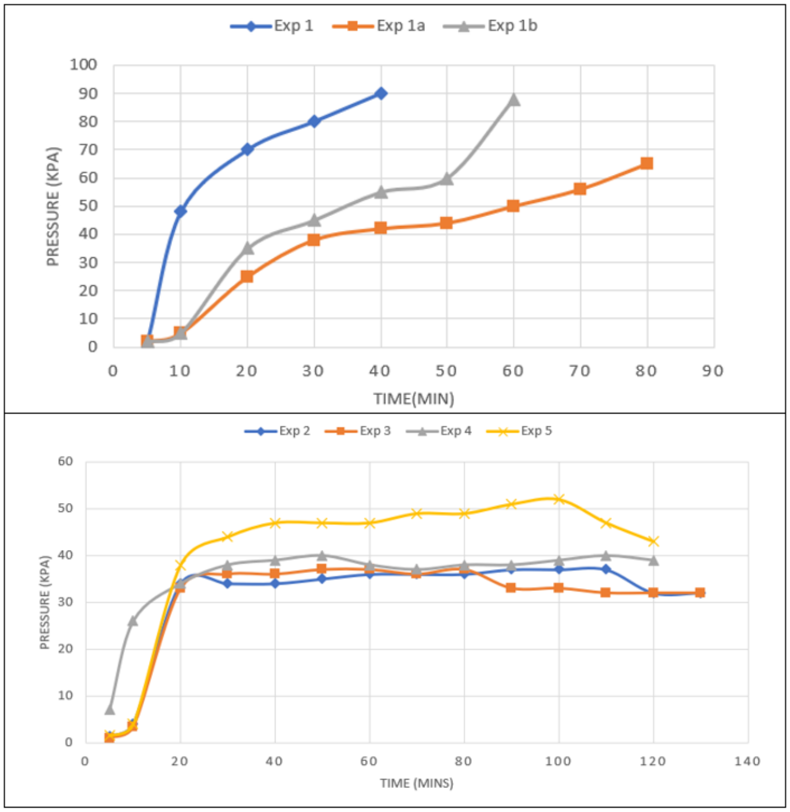

Figure 19 a. The P vs. t graph for the experiments that did not work or got clogged after working for a while, b. The P vs. t graph of the experiments that worked well after the ice bath was added.

The pressure-time graph (Figure 20) and the results for Runs- 2 to 5 prove that the ice bath could assist the tubular reactor configuration in preventing clogging. The two graphs for molecular weight values and the RAA values with time at different initiator loading show how much difference the initiator loading can make when decreased after (<) 0.15M. The molecular weight of Run 5, which is at 0.1M initiator loading, could meet the target spec line of 300kg/mol. Unfortunately, the data we have on Run 5 is only for 90 mins (1.5 hours), but it would be interesting to see the sample results for longer reaction times. With the decrease in the initiator loading, an increase in the RAA values was expected, which can be sought by adding a second stream of the initiator towards the end of the reactor.

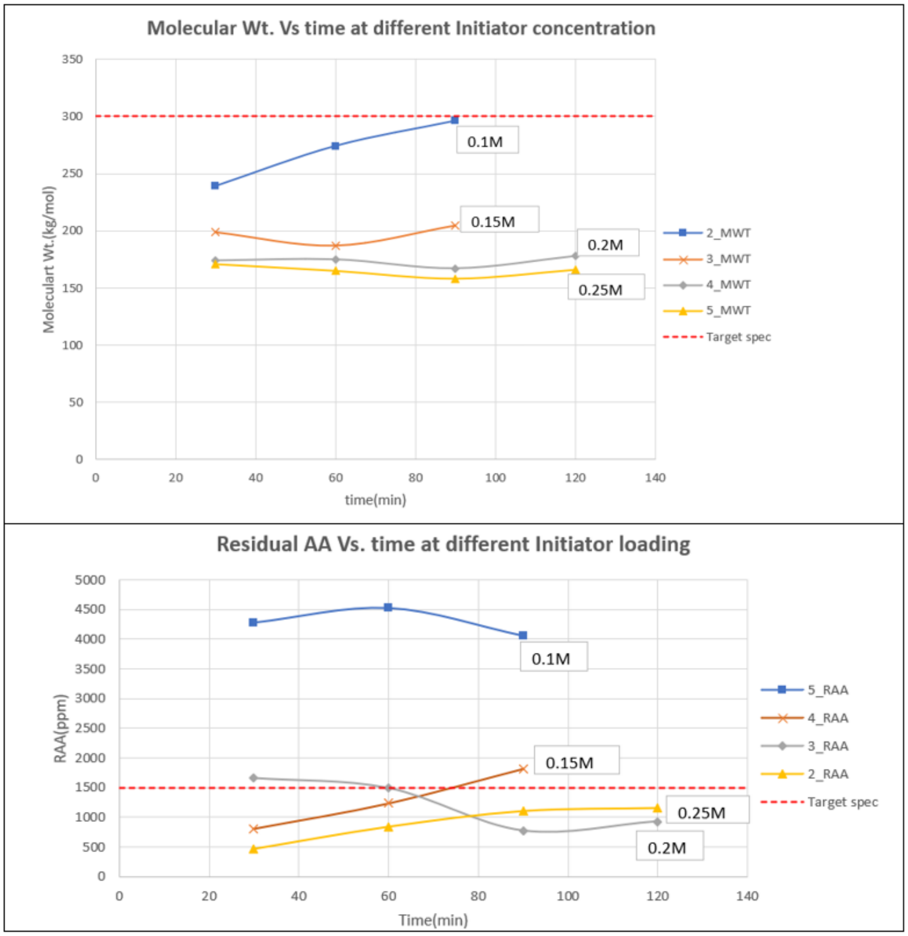

Figure 20 The molecular weight values and the residual acrylic acid values with respect to time with varying initiator loading at around 25%TS and 90^0 C temperature; and at 2.5 min RT.

The last experiment tested the three-monomer feed tubular reactor setup. From the pressure vs. time graph of Run 6 and Run 2 to 5 in the figure, it was observed that the pressure for Run 6 remains low even though the experiment conditions and concentrations were nearly the same. The relative decrease in the pressure for Run 6 makes sense since the monomer concentration for each reactor has decreased and hence the rate of polymer deposition inside the reactor.

This also implies that the three-monomer feed could be a potential setup to ensure safety and thermally better control of the reactions. The results for Run 6 provide a better insight into whether to add a third monomer feed to the setup. The characteristics values of samples collected from both configurations are given in the Table 6 to compare the performance of the two-feed and three-feed tubular reactor.

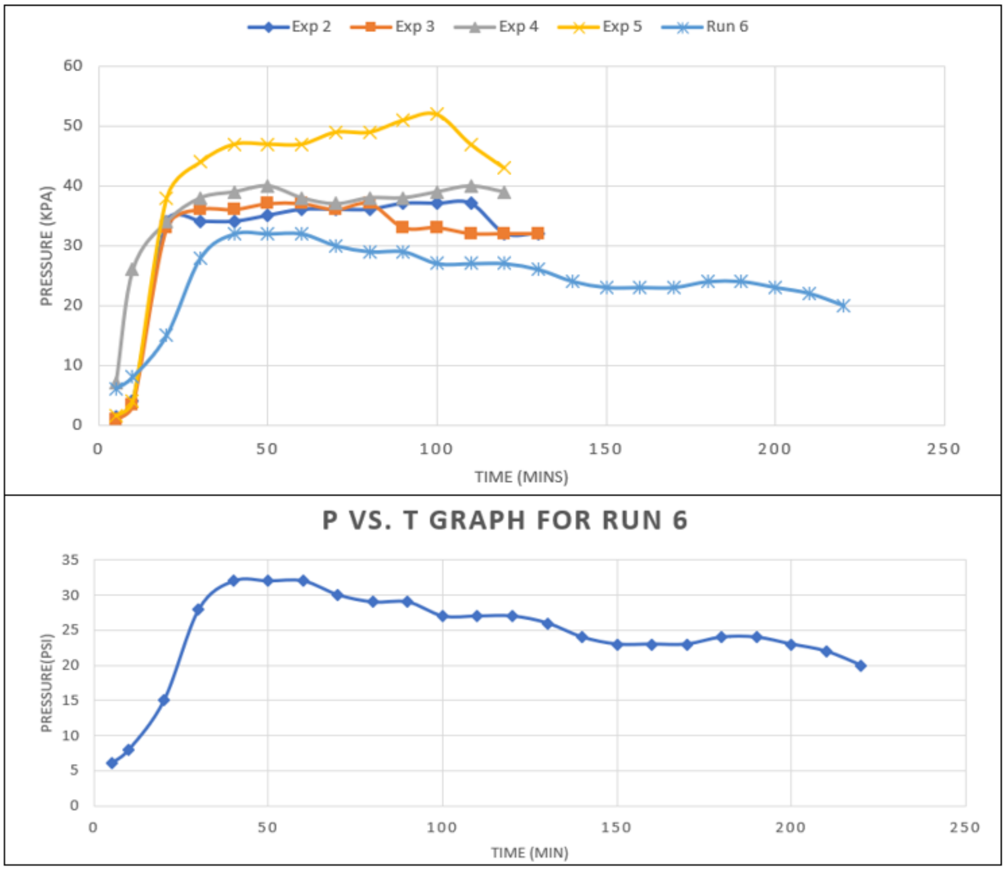

Figure 21a. The pressure vs time graph comparing the pressure lines of experiments conducted on a two-monomer-feed tubular reactor (Run 2 to 5) and a three-monomer feed tubular reactor (Run 6), b. The Pressure vs. time graph for Run 6 conducted on a three monomer-feed tubular reactor configuration.

Both experiments give low molecular weight since the initiator concentration used is high. However, Run 6 gives relatively smaller average molecular weight values as compared to Run3 samples. Run 6 gives a considerably low value for initiator concentration equal to 0.2 M, even though the total solid is 1% less than for Run 3. The reason could be the decrease in the monomer concentration being reacted to per reactor since the monomer feed is not divided into two but three proportions. This can be sought by increasing the monomer concentration or by reducing the initiator concentration which will also reduce the PDI values. Different setups do not seem to impact the PDI values of both experiments, but the RAA values have significantly lowered, resulting in complete conversion for Run 6. From the table below, Run 6 has an initiator-solvent and monomer ratio relatively larger than that of Run 3, hence, the molar mass is expected to be reduced because of an increase in the radical concentration in the stream. However, with reference to that, the PDI was also expected to increase, which is unchanged for Run 3 and 6. The low-pressure results of Run 6 experiment has projected the three-monomer feed reactor as a potential configuration that could operate with more stability and better control, however, more investigation is needed to confirm that.

Table 6 Comparison between the characteristic results of the samples from Experiment Run 3 and 6.

Run	**Reactor Type**	**Total solids %**	**Initiator Concentration (M)**	**Average Molecular Weight (kg/mol)**	**Average Residual Acrylic Acid (ppm)**	**Polydispersity Index**
3	Two monomer feed tubular reactor	25	0.2	173.5	1212	12.4
6	Three monomer feed tubular reactor	24	0.2	142.5	51.25	12.3

5.0 Conclusion

This research has closely met target industrial parameters such as 300,000 g/mol molecular weight, a polydispersity of 10 or below, and a PAA concentration of 25% with 99% conversion via a continuous flow tubular reactor. The work also demonstrates that producing high polymer content PAA, i.e., above 13% TS without the gel effect, is possible if a multiple-monomer feed tubular reactor is used on this lab scale. Whereas, for the initiator concentration, a single feed is adequate even for multiple intermediate-monomer feeds if the residence time is within 1 hour 40 mins (=100 minutes, initiator decay time at 90^0 C). With the help of the vernier pressure graphs on the reactions at different temperatures, it was concluded that for stable operations, the reactor temperature should always be between 85^0 C to 90^0 C, especially when dealing with high monomer concentrations. Also, the estimate of the adiabatic temperature rise of the FRP emphasizes that measures, such as, short residence time, inline static mixers implemented into the streamline, and the monomer-initiator aqueous solution ratio kept below unity, should be implemented in producing high polymer content PAA to prevent thermal runaway. Implementing an ice bath to lower the reaction solution temperature (from the first reactor) before adding the second monomer feed and then passing it through a static mixer just before the second reactor would reduce the chances of the gel effect.

6.0 Future Work

The results obtained from the two-feed tubular reactor configuration were satisfying in terms of delivering desired product quality and stable operations, but these experiments were of limited duration, around 3 to 4 hours long. More investigation of product property variation over time can be done by conducting the same experiments for a longer duration. By making the reactions run longer, other crucial factors can be observed, such as polymer clogging, since the probability of polymer depositions (onto the walls of the tubing) grows over time, especially for higher monomer concentrations. The ice bath feature, which was implemented in the configuration to lower the outflow temperature from the first reactor, can be replaced by a more robust heat removal unit. The investigation of the three-feed tubular reactor configuration is still in its rudimentary stage and requires optimization or better process design. Since experiment 6 has exhibited a low-pressure range of the system throughout the reaction time at around 24%TS, it is worth trying different sets of conditions, preferably a lower initiator (≤ 0.1 M) at higher monomer concentrations, on the three-feed tubular reactor to satisfy the desired product specifications. Also, it would be best to feed the lowest proportion of the monomer concentration at the last inlet feed to account for the unreacted monomer coming from the first and second reactors. Like many research papers, a computation-aided controller can be designed using a mathematical predictive model for optimization and further intensification.

Appendix

Run	T (^{0}C)	RT (min)	Initiator Concentration (M)	Reaction time (min)	Total solids%	Molecular weight (Kg/mol)	Polydispersity Index	RAA (ppm)	Conversion %
2	90	2.5	0.25	30	26.24	171	13.3	469	99.821
				60	25.98	165	12.7	845	99.675
				90	26.19	158	12.1	1111	99.576
				120	25.96	166	12.8	1163	99.552
3	90	2.5	0.20	30	25.37	174	12.2	1658	99.346
				60	25.25	175	12.3	1490	99.410
				90	24.56	167	12.1	772	99.686
				120	24.71	178	13	928	99.624
4	90	2.5	0.15	30	24.15	199	11.2	811	99.664
				60	23.61	187	11.2	1236	99.476
				90	23.62	205	12.2	1815	99.232
5	90	2.5	0.10	30	23.29	239	10.3	4281	98.162
				60	23.49	274	11.8	4527	98.073
				90	23.48	296	12.2	4060	98.271
6	90	2.5	0.20	30	24.80	162	12.85	48	99.981
				60	24.22	140	12.23	56	99.977
				90	23.40	140	12.27	79	99.966
				120	23.00	128	11.9	22	99.990

Bibliography

1. *https://www.themarketreports.com/report/global-polyacrylic-acidpaa-market-research-report*. 2021, The Market Reports.
2. Herth, G., G.D. Schornick, and F.L. Buchholz. *Polyacrylamides and Poly(Acrylic Acids)*. 2015.
3. Abdelaal, M. and M. Makki, *Modification and Characterization of Polyacrylic Acid for Metal Ion Recovery.* American Journal of Polymer Science, 2012. **2**: p. 73-78.
4. Halbe, A.V., et al, *Various applications of acrylics/acrylates in textiles.* 2005. **48**: p. 10-14.
5. Roberts, D.E., *Heats of polymerization - a summary of published values and their relation to structure.* Journal of research of the National Bureau of Standards, 1950. **44**: p. 221.
6. Fujita, M., et al, *Thermal hazard evaluation of runaway polymerization of acrylic acid.* Process Safety and Environmental Protection, 2019.
7. Anxionnaz, Z., et al, *Transposition of an Exothermic Reaction From a Batch Reactor to an Intensified Continuous One.* Heat Transfer Engineering, 2010. **31**: p. 788 - 797.
8. Asua, J.M., *Challenges and Opportunities in Continuous Production of Emulsion Polymers: a Review.* Macromolecular Reaction Engineering, 2016. **10**(4): p. 311-323.
9. Jas, G. and A. Kirschning, *Continuous Flow Techniques in Organic Synthesis.* Chemistry – A European Journal, 2003. **9**(23): p. 5708-5723.
10. Flexible, Fast and Future production processes https://cordis.europa.eu/project/id/228867/reporting
11. Florit, F., et al, *Solution Polymerization of Acrylic Acid Initiated by Redox Couple Na-PS/Na-MBS: Kinetic Model and Transition to Continuous Process.* Processes, 2020.
12. Reis, M.H., F.A. Leibfarth, and L.M. Pitet, *Polymerizations in Continuous Flow: Recent Advances in the Synthesis of Diverse Polymeric Materials.* ACS macro letters, 2020. **9 1**: p. 123-133.
13. Ilare, J., et al, *From batch to continuous free-radical solution polymerization of acrylic acid using a stirred tank reactor.* Reaction Chemistry & Engineering, 2020. **5**(11): p. 2081-2090.
14. Su, Y., Y. Song, and L. Xiang, *Continuous-Flow Microreactors for Polymer Synthesis: Engineering Principles and Applications.* Topics in current chemistry, 2018.
15. Iwasaki, T. and J.-i. Yoshida, *Free Radical Polymerization in Microreactors. Significant Improvement in Molecular Weight Distribution Control.* Macromolecules, 2005. **38**: p. 1159-1163.

16. Qiu, L.-L., et al, *Kinetics study of acrylic acid polymerization with a microreactor platform.* Chemical Engineering Journal, 2016. **284**: p. 233-239.
17. Omidian, H., M.J. Zohuriaan-Mehr, and H. Bouhendi, *Aqueous solution polymerization of neutralized acrylic acid using Na 2 S 2 O 5 /(NH 4) 2 S 2 O 8 redox pair system under atmospheric conditions.* International Journal of Polymeric Materials and Polymeric Biomaterials, 2003. **52**: p. 307 - 321.
18. Hashemi, R., D. Kohlmann, and S. Engell, *Optimizing Control of a Continuous Polymerization Reactor.* IFAC Proceedings Volumes, 2013. **46**: p. 726-731.
19. Chevrel, M.-C., et al, *Continuous Pilot-Scale Tubular Reactor for Acrylic Acid Polymerization in Solution Designed Using Lab-Scale Rheo-Raman data.* Macromolecular Reaction Engineering, 2016. **10**(4): p. 354-363.
20. Micic, N., et al, *Scale-up of the Reversible Addition-Fragmentation Chain Transfer (RAFT) Polymerization Using Continuous Flow Processing.* Processes, 2014. **2**: p. 58-70.
21. Brocken, L., et al, *Continuous flow synthesis of poly(acrylic acid): Via free radical polymerisation.* React. Chem. Eng., 2017. **2**.
22. Costa, C., et al, *Microwave-assisted rapid decomposition of persulfate.* European Polymer Journal, 2009. **45**: p. 2011-2016.
23. Wittenberg, N.F.G., et al, *Modeling Acrylic Acid Radical Polymerization in Aqueous Solution.* Macromolecular Reaction Engineering, 2016. **10**: p. 95-107.
24. Barth, J.V., W. Meiser, and M. Buback, *SP-PLP-EPR Study into Termination and Transfer Kinetics of Non-Ionized Acrylic Acid Polymerized in Aqueous Solution.* Macromolecules, 2012. **45**: p. 1339-1345.
25. Odian,George; *Radical Chain Polymerization*, in *Principles of Polymerization*. 2004. p. 198-349.
26. Lacík, I., et al, *Aqueous phase size-exclusion-chromatography used for PLP-SEC studies into free-radical propagation rate of acrylic acid in aqueous solution.* Macromolecules, 2001. **34**: p. 6224-6228.
27. Acrylic Acid - A summary of safety and handling, B.A.M.M.I., *bamm.net/acrylic-acid-aa/.* . 2018.
28. Chevrel, M.-C., et al, *In situ monitoring of acrylic acid polymerization in aqueous solution using rheo-Raman technique. Experimental investigation and theoretical modelling.* Chemical Engineering Science, 2014. **106**: p. 242-252.

29. Botella, A., et al, *Photo-Rheometry/NIR Spectrometry: An in situ Technique for Monitoring Conversion and Viscoelastic Properties during Photopolymerization.* Macromolecular Rapid Communications, 2004. **25**(12): p. 1155-1158.
30. Kale, L.T. and K.F. O'Driscoll, *Rheokinetics of polymerization of N-laurylmethacrylate.* Polymer Engineering & Science, 1982. **22**(7): p. 402-409.
31. Cutié, S.S., et al, *Acrylic acid polymerization kinetics.* Journal of Polymer Science Part B: Polymer Physics, 1997. **35**(13): p. 2029-2047.
32. Lorber, N., B. Pavageau, and E. Mignard, *Droplet-Based Millifluidics as a New Miniaturized Tool to Investigate Polymerization Reactions.* Macromolecules, 2010. **43**: p. 5524-5529.